JASMAC Conference of the Japan Society of Microgravity Appllication

OR-0710

微小重力/重力下のダストプラズマの分布と相図
Distribution and Phase Diagram of Dusty Plasmas under Microgravity/Gravity

東辻浩夫

Hiroo TOTSUJI

岡山大学 (名誉教授), Okayama University (Prof. Emeritus)

1. Introduction

Dusty plasmas (or fine particle plasmas) are mixtures of weakly ionized plasmas and dust (fine) particles[1)]. Plasmas are usually generated by DC or RF discharge and dust particles (referred to as 'particles' here) are introduced intentionally by particle dispensers. Notations and typical values of parameters are listed in **Table 1**.

gas species	Ar, Ne, etc.
pressure	$p_n = 10 - 10^2$ Pa
temperature	$T_n \sim 300$ K
ion/electron density	$n_i \sim n_e \sim (10^8 - 10^9)$ cm^{-3}
electron temperature	$k_B T_e = (1-3)$ eV
ion temperature	$T_i \sim 300$ K
particle radius	$r_0 \sim (1-10)\mu$m
density	$n_p = (10^4 - 10^5)$ cm^{-3}
temperature	$T_p \sim 300$ K

Table 1 Typical values of parameters.

Particles are negatively charged to large magnitudes around 10^3 times the electron charge. Mutual Coulombic interactions being screened by surrounding plasma with typical screening length of 10^2 μm, they form Yukawa systems. Due to large magnitude of carrying charges, they often provide us with an example of strongly coupled system where individual particles are easily traced. In order to avoid the effects of gravity on macroscopic particles of micron sizes, microgravity experiments have been performed on the ISS[2,3)].

We have analyzed thermodynamics of Yukawa systems and shown a possibility of phase separation and critical phenomena in the domain of very strong coupling[4,5)]. Here we indicate another possibility of phase separation in the domain of strong but not very strong coupling[5,6)].

2. Characteristics of particle distribution

Due to frequent collisions with neutral atoms, distributions of electrons, ions, and particles are described by drift-diffusion equations[7)], From numerical and analytic analyses of distributions of electrons, ions, and particles based on drift-diffusion equations[7–10)], it has been shown that, both under microgravity and gravity, distributions are characterized by

(1) enhancement of charge neutrality in fine particle clouds,

(2) insensitivity of electron distribution to fine particle distribution, and

(3) compensation of negative charge of fine particles by increased ion density.

2.1 Solution of Drift-Diffusion Equation: Cylindrical Symmetry under μg

Figure 1 shows the distributions in the system with the cylindrical symmetry under microgravity[7)]. We clearly observe the above characteristics.

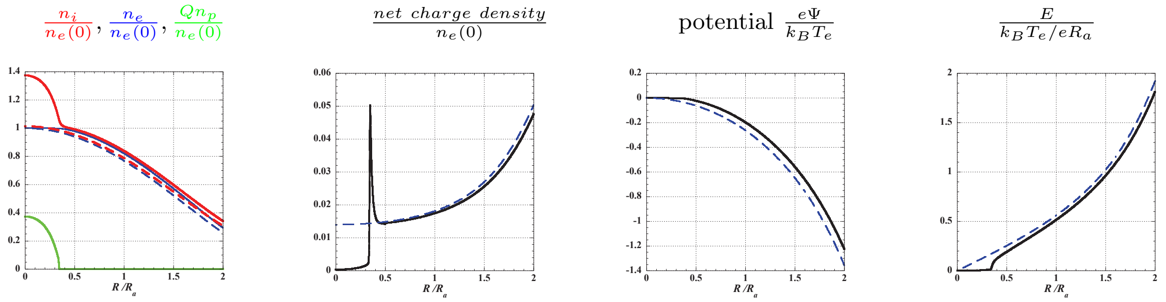

Fig. 1 From left to right: ion (red), electron (blue), and fine particle (green) charge densities; net charge density; potential normalized by $k_B T_e/e$; electric field normalized by $k_B T_e/eR_a$. *Values without fine particles are shown by broken lines.* ($k_B T_e = 1$ eV, $T_i = T_p = T_n = 300$ K, $n_e(0) = 10^8$ cm^{-3}, Ar, $p_n = 40$ Pa, $r_p = 1\mu$m)

2.2 Solution of Drift-Diffusion Equation: One-Dimensional Distribution Cylindrical under g

Under usual gravity on the ground, fine particle clouds are located below the center of the plasma. The distributions of electrons, ions, and particles have to be determined self-consistently so as for the gravity on particles to be balanced by the electric field. An example of distributions is shown in **Figs.2 and 3** [10]. Values of parameters are $T_e = 1$ eV, $T_i = T_p = T_n = 300$ K, $n_e(0) = 10^8$ cm^{-3}, Ar, $p_n = 40$ Pa, and $r_p = 1\mu$m.

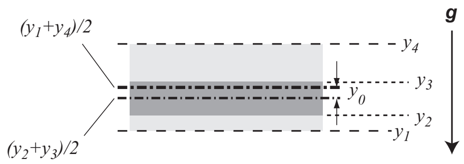

Fig. 2 Plasma (light gray) and fine partcle cloud (dark gray).

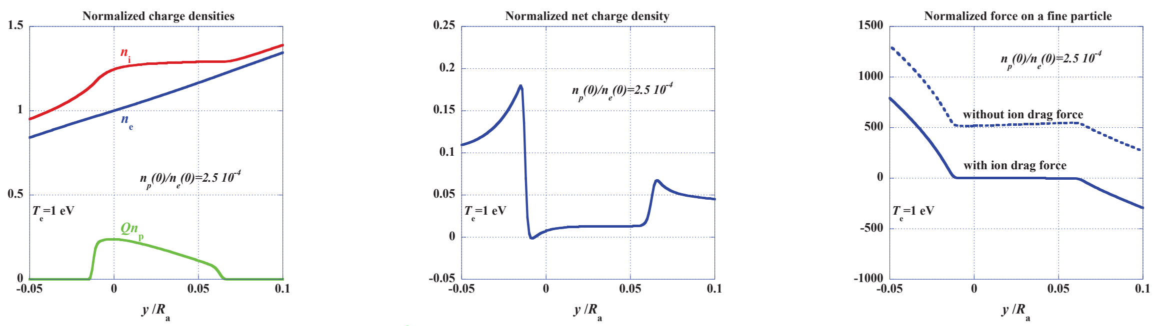

Fig. 3 $\frac{n_i}{n_e(0)}, \frac{n_e}{n_e(0)}, \frac{Qn_p}{n_e(0)}$ (left); $\frac{\text{net charge density}}{n_e(0)}$ (center); $\frac{\text{force on a particle}}{k_B T_e/e^2 R_a}$ (right).

3. Thermodynamics and Phase Diagram

3.1 Helmholtz Free Energy

We have a system of electrons, ions, and particle with (charge, density, temperature), $(-e, n_e, T_e)$, (e, n_i, T_i) and $(-Qe, n_p, T_p)$, where particles interact via the Yukawa interaction $\frac{(Qe)^2}{4\pi\varepsilon_0 r}\exp\left(-\frac{r}{\lambda}\right)$. Yukawa system is characterized by parameters, $a = (3/4\pi n_p)^{1/3}$ being the mean distance,

$$\Gamma = \frac{(Qe)^2}{4\pi\varepsilon_0 a k_B T_p}, \tag{1}$$

$$\xi = \frac{a}{\lambda}. \tag{2}$$

The Helmholtz free energy is written as

$$F = F_{\rm id}^{(e)}(T_e, V, N_e) + F_{\rm id}^{(i)}(T_i, V, N_i) + F_{\rm id}^{(p)}(T_p, V, N_p) + N_p k_B T_p f^{(p)}, \tag{3}$$

where $N_{e,i,p} = n_{e,i,p}V$, $F_{\rm id}^{(e,i,p)}$ the ideal gas value, and $N_p k_B T_p f^{(p)}$ the non-ideal part. From Yukawa numerical simulations, we have an interpolation formula for $f^{(p)}$ [4]

$$f^{(p)}(\tilde{\Gamma}, \xi, \tilde{r}_p) \approx a_1 \tilde{\Gamma} \exp(a_2 \xi) + 4a_3 \tilde{\Gamma}^{1/4} \exp(a_4 \xi) + \frac{3}{2}\tilde{\Gamma}\xi^{-2}[1-(1+2\tilde{r}_p)\exp(-2\tilde{r}_p)] - \frac{1}{2}\tilde{\Gamma}\xi(1+\tilde{r}_p)\exp(-2\tilde{r}_p), \quad (4)$$

where

$$\tilde{\Gamma} = \Gamma \frac{\exp(2\tilde{r}_p)}{(1+\tilde{r}_p)^2}, \ \tilde{r}_p = \frac{r_p}{\lambda}, \ a_1 = -0.896, \ a_2 = -0.588, \ a_3 = 0.72, \text{ and } a_4 = -0.22.$$

Parameters $\tilde{\Gamma}/\Gamma$ and $\tilde{r}_p$ express the effects of finite particle radius r_p ($\tilde{\Gamma} = \Gamma$ and $\tilde{r}_p = 0$ for $r_p = 0$).

3.2 Condition for Chemical Potential

When $n_e \approx n_i \gg Qn_p$, particles can be regarded as solute in background plasma and we have a possibility of coexisting phases with different particle densities [5,6]. Denoting the non-ideal part of particle chemical potential by $\Delta\mu^{(p)}$, we have the condition for coexisting phases, I and II, as [11]

$$k_B T_p \ln \frac{n_p^I}{n_p^{II}} + Qk_B T_i \ln \frac{n_e^I + Qn_p^I}{n_e^{II} + Qn_p^{II}} = -\left[\Delta\mu^{(p)}\right]^I + \left[\Delta\mu^{(p)}\right]^{II}, \quad (5)$$

$$\frac{\Delta\mu^{(p)}}{k_B T_p} = \frac{1}{3} a_1 \tilde{\Gamma} \exp(a_2\xi)(4 - a_2\xi) + \frac{1}{3} a_3 \tilde{\Gamma}^{1/4} \exp(a_4\xi)(13 - 4a_4\xi)$$
$$+ 3\tilde{\Gamma}\xi^{-2}[1-(1+2\tilde{r}_p)\exp(-2\tilde{r}_p)] - \frac{1}{2}\tilde{\Gamma}\xi(1+\tilde{r}_p)\exp(-2\tilde{r}_p). \quad (6)$$

The critical condition for effective chemical potential is $\dfrac{\partial\tilde{\mu}}{\partial n_p} = 0$, where

$$\tilde{\mu} = k_B T_p \ln n_p + Qk_B T_i \ln(n_e + Qn_p) + \Delta\mu^{(p)}. \quad (7)$$

Here the second term of $\tilde{\mu}$ comes from the charge neutrality condition.

We note that, when n_p changes (with n_e and n_i kept unchanged), $\Gamma\xi \approx$ const as

$$\Gamma\xi \approx \frac{(4\pi n_e)^{1/2} Q^2 e^3}{k_B T_p (k_B T_i)^{1/2}} = \text{const} \sim 5.5 \cdot 10 \frac{(k_B T_e[\text{eV}])^2 (r_p[\mu\text{m}])^2 \left(n_e/10^8 \text{ cm}^{-3}\right)^{1/2}}{(T_p/300 \text{ K})\,(T_i/300 \text{ K})^{1/2}}. \quad (8)$$

Here we have estimated the value of Q by

$$Q \sim 0.5 \frac{k_B T_e}{e^2/4\pi\varepsilon_0 r_p} \sim 3.5 \cdot 10^2 (k_B T_e[\text{eV}]) r_p[\mu\text{m}].$$

Values of $\Gamma\xi$ cover a wide range: When $n_e \sim 10^8$ cm^{-3} with $k_B T_e \sim (1\text{–}3)$ eV and $r_p \sim (1\text{–}3)$ μm, $\Gamma\xi \sim (5.5 \cdot 10 - 4.5 \cdot 10^3)$, and, when $n_e \sim 8 \cdot 10^8$ cm^{-3}, $\Gamma\xi \sim (1.6 \cdot 10^2 - 1.3 \cdot 10^4)$.

3.3 Phase Diagrams

Example of the behavior of $\tilde{\mu}$ along $\Gamma\xi$ = const. = C are shown in **Fig.4**. The appearance of extrema signals phase coexistence. An example of the phase diagram is shown in **Fig.5(left)**: For $\Gamma\xi < (\Gamma\xi)_c$, we have one phase, for $\Gamma\xi = (\Gamma\xi)_c$, we have a critical point at (Γ_c, ξ_c), and for $\Gamma\xi > (\Gamma\xi)_c$, we have both one-phase and two-phase domains. The dependence of Γ_c and ξ_c on $\tilde{r}_p = r_p/\lambda$ is shown in **Fig.5(right)** and approximately given by

$$\Gamma_c \approx 3.74 \cdot 10^2 - 94.5\, \tilde{r}_p + 5.63 \cdot 10^3\, \tilde{r}_p^2, \ \xi_c \approx 5.11 + 0.15\, \tilde{r}_p + 2.3\, \tilde{r}_p^2$$

4. Conclusion and Discussion

It has been shown that there exists a possibility of *thermodynamic* separation of fine particle cloud into high and low density parts (phases). Density ratio can be of the order of 10. Necessary condition is strong but not very strong coupling between fine particles.

The above condition seems to be not difficult to realize in experiments with the apparatus PK-4 on the ISS [2]. We also note that, under the gravity on the ground, these thermodynamic separations might appear in the horizontal structures of fine particle clouds. In the latter case, one should be careful to avoid the effects of ion flow which is believed to play a significant role in the formation of the void [12].

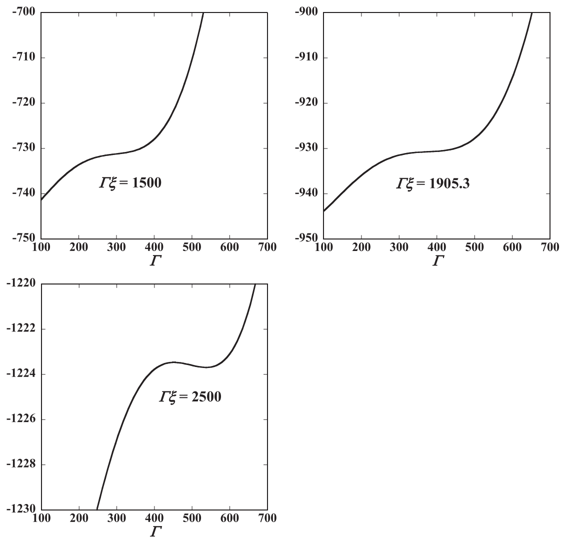

Fig. 4 $\tilde{\mu}/k_B T_p$ on $\Gamma\xi = C$ with $\tilde{r}_p = 8.37 \cdot 10^{-3}$; $(\Gamma\xi)_c = 1905.3$, $\Gamma_c = 373.0$, and $\xi_c = 5.11$. (The origin of ordinate is arbitrarily shifted.)

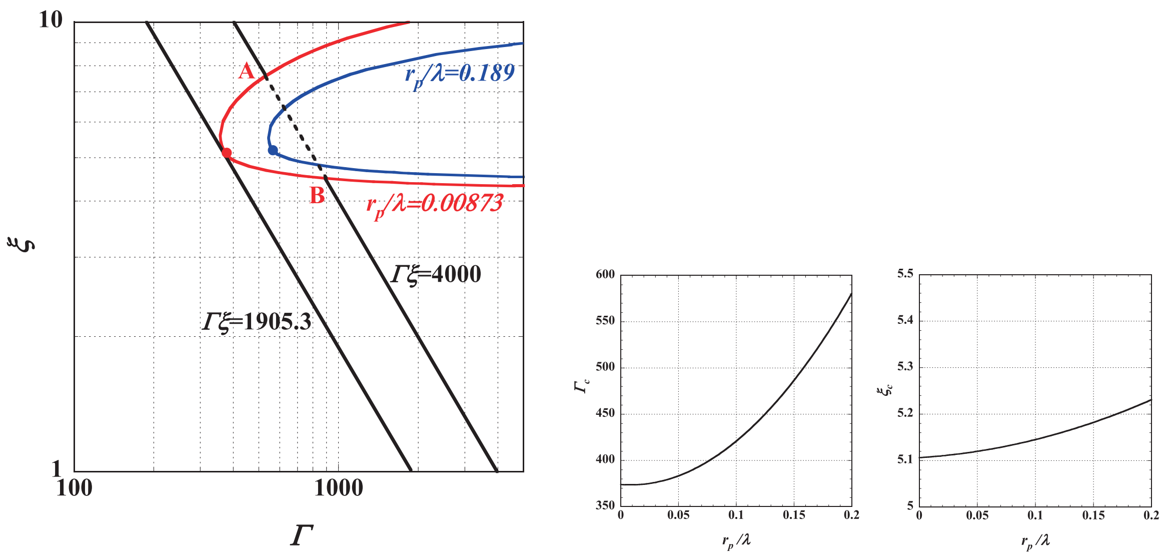

Fig. 5 Left: $\tilde{r}_p = 8.73 \cdot 10^{-3}$ (e.g., $r_p = 1\ \mu$m, $n_e = 10^8$ cm^{-3}) and $\tilde{r}_p = 1.89 \cdot 10^{-1}$(e.g., $r_p = 8\ \mu$m, $n_e = 8 \cdot 10^8$ cm^{-3}). Filled circles are critical points. For $\tilde{r}_p = 8.73 \cdot 10^{-3}$ and $\Gamma\xi = 4000$, two phases (A and B) coexist between A and B. Right: Dependence of Γ_c and ξ_c on $\tilde{r}_p = r_p/\lambda$.

References

1) For example, P. K. Shukla and A. A. Mamun, *Introduction to Dusty Plasma Physics* (Institute of Physics Publishing, London, 2002).

2) For example, V. Fortov, G. Morfill, O. Petrov, M. Thoma, A. Usachev, H. Höfner, A. Zobin, M. Kretschmer, S. Ratynskaia, M. Fink, K. Tarantik, Yu. Gerasimov, and V. Esenkov, Plasma Phys. Control. Fusion **47**, B537(2005).

3) For example, H. M. Thomas, G. E. Morfill, V. E. Fortov, A. V. Ivlev, V. I. Molotkov, A. M. Lipaev, T. Hagl, H. Rothermel, S. A. Khrapak, R. K. Suetterlin, M. Rubin-Zuzic, O. F. Petrov, V. I. Tokarev, and S. K. Krikalev, New J. Phys. **10**, 033036(2008).

4) H. Totsuji, Phys. Plasmas **15**, 072111 (2008).

5) H. Totsuji, Microgravity Sci. Techno. **23**, 159 (2011).

6) H. Totsuji, Microgravity Sci. Techno. **32**, 699 (2020).

7) H. Totsuji, Plasma Phys. Control. Fusion **58**, 045010 (2016).

8) H. Totsuji, Phys. Letters A **380**, 1445(2016).

9) H. Totsuji, Phys. Letters A **381**, 903(2017).

10) H. Totsuji, J. Phys. Commun. **2**, 025023 (2018).

11) For example, L. D. Landau and E. M. Lifshitz, *Statistical Physics, 3rd Edition, Part I*, Section 97 (Pergamon, Oxford, 1980).

12) For example, J. Goree, G. E. Morfill, V. N. Tsytovich, and S. V. Vladimirov, Phys. Rev. E **59**, 7055 (1999).